

Near Field Shielding of a Wireless Power Transfer (WPT) Current Coil

Mauro Feliziani^{1, *}, Silvano Cruciani¹, Tommaso Campi¹, and Francesca Maradei²

Abstract—The configuration of an infinite planar conductive shield is examined when it is excited by an electromagnetic near field generated by a coil current source as that of a wireless power transfer (WPT) system. The analytical expressions of the electromagnetic field based on the transmission theory of shielding are given for different frequencies and different incidence angles of the near field generated by the coil current, assuming the conductive planar shield placed in the close proximity of the coil. The obtained results are discussed and compared with other traditional analytical and numerical solutions.

1. INTRODUCTION

Low frequency shielding is traditionally a hot topic since the magnetic field is considered a critical issue in terms of both Electric and Magnetic Field (EMF) safety and Electromagnetic Compatibility/Electromagnetic Interference (EMC/EMI). In the past, great attention was addressed to extremely low frequency (ELF) applications due to the public concern for human exposure to magnetic fields, especially after the 2002 IARC classification of power frequency magnetic fields as possibly carcinogenic to humans (Group 2B). This concern is even amplified by the difficulties in mitigating low frequency magnetic fields [1–12].

Nowadays, growing interest is directed to EMF safety concerns about magnetic fields in applications related to the emerging technology of the Wireless Power Transfer (WPT) based on magnetic resonant coils [13–20]. WPT for battery recharging is spreading in a number of applications such as automotive, biomedical devices, and consumer electronics. In future perspective, we can envision the progressive substitution of the power wiring systems with wireless links based on inductive coupling. It means that humans and electrical/electronic devices will be exposed to magnetic fields at frequencies in the range between a few kilohertz and tens of megahertz.

For the aforementioned reasons, there is big renovated interest for low-frequency low-impedance electromagnetic shielding in case the source is given by a current flowing into a coil at frequencies higher than the power frequency. This simple configuration can be seen as the basis for the calculation method of WPT multicoil/multiturn systems.

Near-field shielding has been investigated for many years [1–9], but the analytical expressions given in [2, 3] are very complex and not very accurate at higher frequencies because the axial variation of eddy currents within the shield is neglected, so industry engineers and technicians often prefer to deal with numerical studies instead of solving difficult analytical equations. However, the numerical approach based on the solution of partial differential equations (PDE) is not an easy task at the higher frequencies when the penetration depth inside the conductive shield region is so much smaller than the shield thickness, and solution of a three-dimensional shielding configuration requires heavy computations.

Received 28 April 2017, Accepted 8 August 2017, Scheduled 21 August 2017

* Corresponding author: Mauro Feliziani (mauro.feliziani@univaq.it).

¹ Department of Industrial and Information Engineering, University of L'Aquila, L'Aquila, Italy. ² Department of Astronautics, Electrical and Energetic Engineering, Sapienza University of Rome, Rome, Italy.

To overcome this inconvenience, the transmission theory of shielding is here applied to evaluate the shielding effectiveness of a planar conductive shield when it is excited by the near field generated from a circular loop current. This method, known also as transmission line (TL) method, is not based on the solution of partial differential equations (PDE) as in [2, 3], but based on the adaptation of the classical shielding theory proposed in [1, 5, 6, 9] to the case of a current coil above a planar shield. The TL method for shielding is based on the solution of telegraphers' equations in terms of field quantities to account the quasi TEM field propagation inside a highly conductive shield barrier. For plane wave excitation, the TL terminations are given in terms of wave impedances calculated as the ratio between the tangential components of electric and magnetic incident fields. For near-field sources, the field in air is quasi stationary, and the TL is terminated on impedances which are not always identical to the wave impedances of the incident field. The use of realistic values of wave impedances as TL terminations is a key point in the adaptation of the TL method to near-field shielding problems. In the past, several authors used, as TL terminations in near field applications, the wave impedances of the incident field as usually done for far-field methods; however, this solution produces accurate results only in the axial direction of the circular coil [3, 5], but not in the radial direction which is very important in some applications as WPT. Here, the TL method for near-field shielding is reviewed and improved to achieve good accuracy in a wide frequency range and for different values of the radial distance. The accuracy of the TL method has been significantly increased by applying a suitable expression of the wave impedance used as terminal load of the equivalent TL. In the following sections, the mathematical method is described and discussed. Then some applications are presented to show the advantages and disadvantages of the proposed method compared with other analytical and numerical techniques. Finally, it should be pointed out that this procedure is completely analytical and based on TL/circuit approach. Thus, the proposed method is very different from Impedance Network Boundary Conditions (INBCs) [24–27] or similar approaches that have been utilized to eliminate the shield from the computational domain in PDE numerical solution in order to reduce the computational cost.

2. MATHEMATICAL METHOD

2.1. System Configuration

The configuration under examination is given by an infinite planar conductive shield excited by a magnetic near field produced by a current loop of radius R . The planar loop and conductive shield of thickness t are parallel, both lying in the xy plane and separated by a distance d , as shown in Fig. 1. The coil is assumed to be in free space, and the planar shield is composed of a linear lossy material with specific constants σ , $\varepsilon = \varepsilon_r \varepsilon_0$, $\mu = \mu_r \mu_0$, with σ being the conductivity and ε_r and μ_r the relative permittivity and permeability, respectively. The wire is assumed to be very thin, and the small loop approximation is adopted, i.e., time-harmonic current $I = I_\varphi$ is constantly distributed in the coil. The configuration under study is suitable to be modeled by a 2D axially symmetrical domain using cylindrical coordinates (ρ, φ, z) . The only non-zero field components are E_φ , H_ρ and H_z , whose expressions are analytically known in free space [21–23]. The field created by the current loop in free space is assumed to be the incident field (i.e., field in the absence of the shield) on the planar shield.

2.2. Field Propagation inside Conductive Shield

Some simplifying assumptions are made in the present study. The infinite planar shield of thickness t is considered composed by a good conductor material ($\sigma \gg \omega\varepsilon$). It means that the displacement currents are negligible in comparison with conductive currents. This assumption is valid at any frequency for many practical WPT applications when considering metal shields, e.g., made with aluminum or copper.

Another relevant assumption is that the tangential components of the electromagnetic field inside the conductive shield propagate in the direction ζ perpendicular to the shield surfaces Γ_0 and Γ_t , and therefore, the refraction angle is assumed to be zero [9]. This approximation can be successfully used for a large value of σ as that of metals. Thus, the propagation of the field tangential components inside the shield barrier can be modeled by the TL theory of shielding, i.e., plane wave propagation described by telegraphers' equations in terms of transversal components of electric and magnetic fields. This approach is well described in [9] for spatially constant incident fields and is widely used for plane

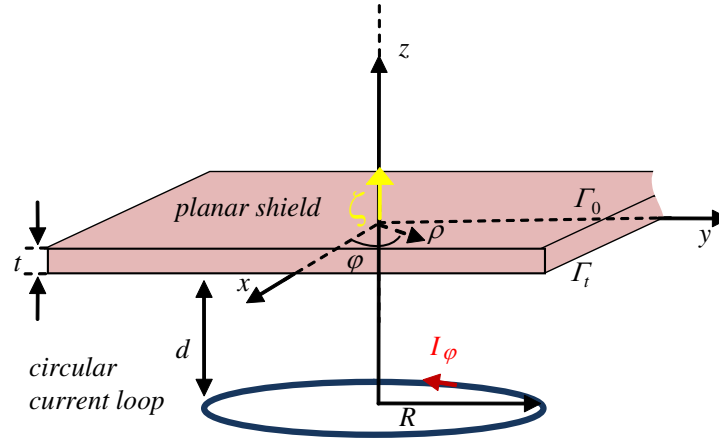


Figure 1. System configuration.

wave incident fields with any incidence angle. Here, this approach is assumed to be valid at any point on the shield surfaces for a spatially varying incident field as that created by a current loop. Thus, the TL equations in terms of tangential components of electric and magnetic fields, E_φ and H_ρ , which depend on cylindrical coordinates ρ , $\zeta = z - d$ and independent of φ due to axial symmetry, are given for $t \geq \zeta \geq 0$ by:

$$\frac{dE_\varphi(\rho, \zeta)}{d\zeta} = j\omega\mu H_\rho(\rho, \zeta) \quad (1)$$

$$\frac{dH_\rho(\rho, \zeta)}{d\zeta} = (\sigma + j\omega\varepsilon) E_\varphi(\rho, \zeta) \approx \sigma E_\varphi(\rho, \zeta) \quad (2)$$

By a simple mathematical treatment, the tangential components of the electric and magnetic fields at both sides of the solid planar shield ($E_{\varphi 0}(\rho)$ and $H_{\rho 0}(\rho)$ on Γ_0 at $\zeta = 0$; $E_{\varphi t}(\rho)$ and $H_{\rho t}(\rho)$ on Γ_t at $\zeta = t$) are related by the following equations:

$$E_{\varphi 0}(\rho) = \cosh(\gamma_s t) E_{\varphi t}(\rho) + \eta_s \sinh(\gamma_s t) H_{\rho t}(\rho) \quad (3)$$

$$H_{\rho 0}(\rho) = \frac{\sinh(\gamma_s t)}{\eta_s} E_{\varphi t}(\rho) + \cosh(\gamma_s t) H_{\rho t}(\rho) \quad (4)$$

where η_s and γ_s are the spatially constant intrinsic impedance and propagation constant of the shield, given for a good conductor by:

$$\eta_s = \sqrt{\frac{j\omega\mu}{\sigma}} \quad (5)$$

$$\gamma_s = \sqrt{j\omega\mu\sigma} \quad (6)$$

To determine the field tangential components in Eq. (2), it is necessary to apply boundary conditions (BCs). This problem can be modeled by an equivalent circuit, where the shield is modeled by a lossy TL when considering distributed parameter circuit as shown in Fig. 2(a), or by a T -type lumped parameter equivalent circuit as shown in Fig. 2(b). The BCs are modeled as circuit terminations. Traditionally, the terminal loads are the wave impedances $Z_{w0}(\rho)$ and $Z_{wt}(\rho)$ that depend only on the source configuration, while the series impedance Z_s and shunt impedance Z_a are spatially constant since they depend at a given frequency only on the shield characteristics (i.e., thickness, material, etc.), and their expressions are given by [9]:

$$Z_s = \eta_s \frac{\cosh(\gamma_s t) - 1}{\sinh(\gamma_s t)} \quad (7)$$

$$Z_a = \eta_s \frac{1}{\sinh(\gamma_s t)} \quad (8)$$

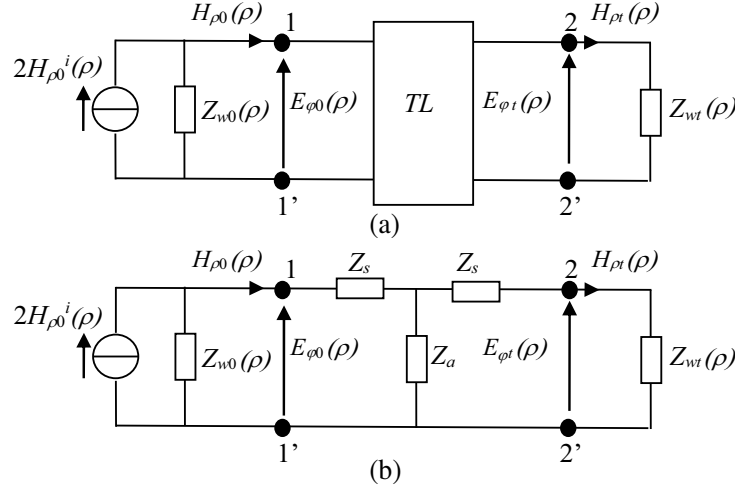


Figure 2. Equivalent TL configuration for a near field incident to a conductive shield. (a) Distributed parameter equivalent circuit. (b) Lumped parameter equivalent circuit.

Note that in the equivalent circuit of Fig. 2, the two-port network representing the shield is spatially constant when considering a solid planar shield, while the terminations, $H_{\rho 0}^i(\rho)$, $Z_{w0}(\rho)$ and $Z_{wt}(\rho)$, spatially vary depending on the source configuration.

The circuit excitation is given by Norton equivalent representation as an independent current source function of the incident magnetic field $H_{\rho}^i(\rho, 0)$ at $\zeta = 0$ in parallel with the wave impedance $Z_{w0}(\rho)$. Both source and wave impedance can be obtained analytically. In the traditional application of the TL method for shielding, the right terminal wave impedance is given by the ratio of the tangential components of the incident fields, but this approach does not achieve good results [3]. Here a significant modification is carried out modifying the right terminal load $Z_{wt}(\rho)$ at $\zeta = t$ which is assumed to be the ratio of the tangential components of the total fields instead of the incident fields. Thus the two terminal impedances, $Z_{w0}(\rho)$ at $\zeta = 0$ and $Z_{wt}(\rho)$ at $\zeta = t$, are given for a circular current loop by [2]:

$$Z_{w0}(\rho) = \frac{-E_{\varphi 0}^i(\rho)}{H_{\rho 0}^i(\rho)} = \frac{j\omega\mu_0 2R\rho\alpha^2 [(2-p)K(p) - 2F(p)]}{dp [(R^2 + \rho^2 + d^2)F(p) - \alpha^2 K(p)]} \quad (9)$$

and

$$Z_{wt}(\rho) = \frac{-E_{\varphi t}(\rho)}{H_{\rho t}(\rho)} = -j\omega \frac{\int_0^{\infty} \frac{C\lambda\tau}{\tau_0} J_1(\lambda R) J_1(\lambda\rho) e^{-\tau_0 d - t(\tau - \tau_0)} d\lambda}{\int_0^{\infty} \frac{C\lambda\tau}{\tau_0^2} J_1(\lambda R) J_1(\lambda\rho) e^{-\tau_0 d - t(\tau - \tau_0)} d\lambda} \quad (10)$$

when F and K are elliptical integrals with argument $p = 1 - (\alpha/\beta)^2$ and when posing $\alpha^2 = R^2 + \rho^2 + d^2 - 2R\rho$, $\beta^2 = \alpha^2 + 4R\rho$ while J_ν is the Bessel integral function of first kind with $\nu = 1$, $\tau = \sqrt{\lambda^2 - j\omega\mu\sigma}$, $\tau_0 = \sqrt{\lambda^2 - \omega^2\mu_0\varepsilon_0}$, $C = ((\tau/\tau_0 + \mu_r)^2 - (\tau/\tau_0 - \mu_r)^2 e^{-2t\tau})^{-1}$.

The input impedance $Z_{i0}(\rho)$ seen at the circuit port 1-1' (see Fig. 2) is given by:

$$Z_{i0}(\rho) = Z_s + Z_a \frac{Z_s + Z_{wt}(\rho)}{Z_a + Z_s + Z_{wt}(\rho)} \quad (11)$$

It should be noted that for many practical shielding configurations for WPT systems $|\eta_s| < |Z_{i0}(\rho)| \ll |Z_{w0}(\rho)|, |Z_{wt}(\rho)|$. It means that the TL termination is a high impedance load, and therefore, a significant reflection of the tangential fields occurs.

The tangential components of the electric and magnetic fields on Γ_0 at $\zeta = 0$ are then obtained via circuit analysis by:

$$H_{\rho 0}(\rho) = \frac{Z_{w0}(\rho)}{Z_{w0}(\rho) + Z_{i0}(\rho)} 2H_{\rho 0}^i(\rho) \quad (12)$$

$$E_{\varphi 0}(\rho) = \frac{Z_{i0}(\rho)Z_{w0}(\rho)}{Z_{w0}(\rho) + Z_{i0}(\rho)} 2H_{\rho 0}^i(\rho) \quad (13)$$

From the knowledge of $E_{\varphi 0}(\rho)$ and $H_{\rho 0}(\rho)$ the tangential fields $E_{\varphi t}(\rho)$ and $H_{\rho t}(\rho)$ on Γ_t at $\zeta = t$ can be simply derived via Eqs. (3)–(4). By simple manipulations, the ratio between the incident and the shielded magnetic fields at any point ρ on Γ_t can be obtained as:

$$\frac{H_{\rho t}^i(\rho)}{H_{\rho t}(\rho)} = \frac{Z_{w0}(\rho) + Z_{i0}(\rho)}{2Z_{w0}(\rho) (-Z_{i0}(\rho) \sinh(\gamma_s t) / \eta_s + \cosh(\gamma_s t))} \quad (14)$$

By the analysis of the equivalent circuit, it is possible to accurately evaluate the tangential components of the magnetic field, $H_{\rho t}$, and of the electric field, $E_{\varphi t}$, behind the shield. The problem still to be solved is the evaluation of the normal component of the magnetic field, H_z . This component can be simply evaluated via the magnetic vector potential $\mathbf{A} = A_\varphi \hat{\varphi}$ [2]. In fact, E_φ is the only non-zero component of the electric field \mathbf{E} and is given by

$$E_\varphi = -j\omega A_\varphi, \quad (15)$$

and the magnetic field related to the magnetic vector potential given by

$$\mathbf{H} = H_\rho \hat{\rho} + H_z \hat{\mathbf{z}} = \frac{1}{\mu} \nabla \times \mathbf{A}, \quad (16)$$

thus, the normal component of the magnetic field, H_z , is derived as:

$$H_z = \frac{1}{\mu} (\nabla \times \mathbf{A})_z = \frac{1}{\mu} (\nabla \times A_\varphi \hat{\varphi})_z = \frac{1}{\mu} \left(\frac{\partial A_\varphi}{\partial \rho} + \frac{1}{\rho} A_\varphi \right) \quad (17)$$

or in terms of the electric field E_φ as

$$H_z = -\frac{1}{j\omega\mu} \left(\frac{\partial E_\varphi}{\partial \rho} + \frac{1}{\rho} E_\varphi \right) \quad (18)$$

Equation (18) can be easily calculated when the electric field distribution is known, that is exactly our case in which the electric field is obtained by the solution of the equivalent circuit in Fig. 2.

The shielding effectiveness of the magnetic field, SE_H , in decibels (dB), can be calculated by:

$$SE_H(\rho) = 20 \log_{10} \frac{|H_t^i(\rho)|}{|H_t(\rho)|} \quad (19)$$

where $H_t^i(\rho)$ is the incident magnetic field (i.e., field in absence of the shield), and $H_t(\rho)$ is the total magnetic field in presence of the shield, both calculated at $\zeta = t$. Thus SE_H is finally given by

$$SE_H(\rho) = 20 \log_{10} \left(\frac{\sqrt{|H_{\rho t}^i(\rho)|^2 + |H_{z t}^i(\rho)|^2}}{\sqrt{|H_{\rho t}(\rho)|^2 + |H_{z t}(\rho)|^2}} \right) \quad (20)$$

3. APPLICATIONS

The proposed analytical solution is approximate, and its accuracy is strongly dependent on the ratio δ/t , with $\delta = (\pi\mu\sigma f)^{-1/2}$ being the penetration depth and f the frequency. The behavior of the ratio δ/t vs. frequency is shown in Fig. 3 for copper and aluminum planar shields when assuming $t = 1$ mm.

The electro-geometrical configuration of a circular coil with radius $R = 50$ mm and carrying a unit current $I = I_\varphi$ is considered. The coil is assumed to be parallel to an infinite copper shield of thickness $t = 1$ mm at distance $d = 10$ mm, as shown in Fig. 4. The frequency behavior of SE_H is evaluated at

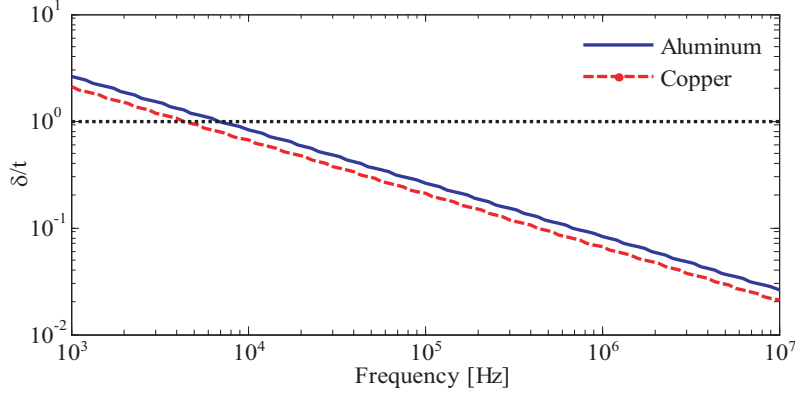


Figure 3. Behavior of the ratio δ/t vs. the frequency for $t = 1$ mm.

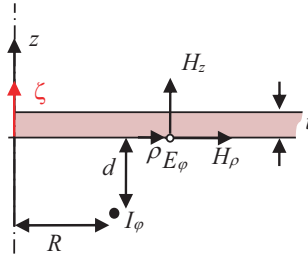


Figure 4. 2D axially symmetrical configuration of a circular current loop above a planar shield.

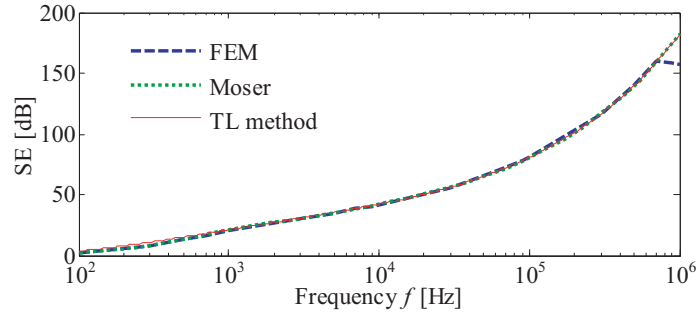


Figure 5. Magnetic shielding effectiveness SE_H of a copper plate at $\rho \approx 0$ for $d = 20$ mm and $t = 1$ mm.

the center of the coil on Γ_t ($\rho = 0$, $\zeta = t$). The obtained results are shown in Fig. 5 and compared with the numerical solutions obtained by a FEM code and the method proposed by Moser [2]. All the considered methods produce almost identical solutions. The FEM solution has been achieved analyzing the 2D axially symmetrical configuration using the same fixed mesh for all the considered frequencies. Thus, the FEM solution is not accurate at the higher frequencies since the mesh discretization is not fine enough to suitably model the field propagation through the conductive shield.

The tangential components of the magnetic field, H_ρ , are calculated along the radial distance ρ at $\zeta = t$ at four different frequencies, 100 Hz, 1 kHz, 10 kHz and 100 kHz, of relevant interest for power and WPT automotive applications [15, 16]. The results are obtained considering a copper shield with $t = 1$ mm and coil/shield separation $d = 10$ mm, as shown in Fig. 6. The tangential components of the electric field, E_φ , and the normal component of the magnetic field, H_z , calculated for the same configuration previously described, are shown in Figs. 7 and 8. The shielding effectiveness SE_H is also reported in Fig. 9. The results obtained by the proposed TL method are compared with Moser's method [2] and with the reference solution obtained numerically by the FEM. As can be observed, the solutions of the proposed method is very accurate, and its accuracy increases as the frequency increases,

while the trend of Moser’s method solution is the opposite, as described in [3]. At the lowest frequency of 100 Hz which is a very low value and comparable with the power frequency, when the validity of the TL method is doubtful, the error in SE_H obtained by the proposed method is within 3 dB. Finally, it should be noted that the error decreases as the separation d between shield and coil increases.

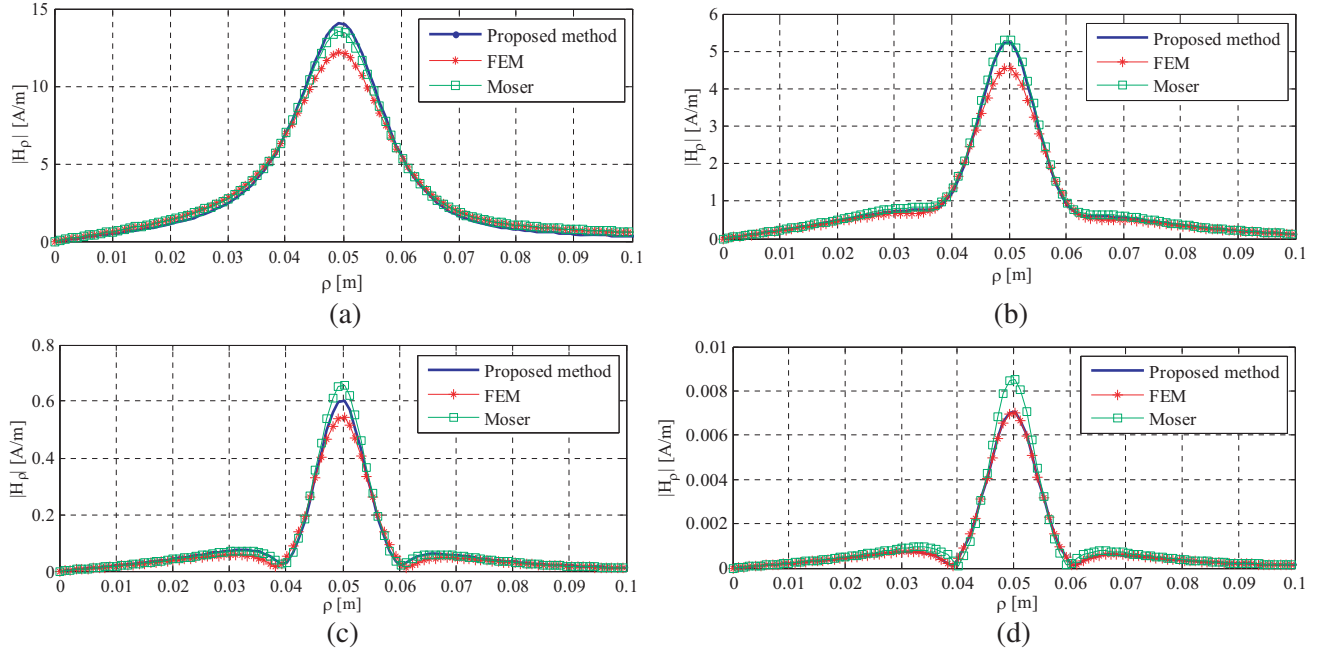


Figure 6. Complex magnitude of magnetic field tangential component H_ρ calculated at $\zeta = t$ for various frequencies along the radial distance ρ assuming $d = 10$ mm and $t = 1$ mm. (a) $f = 100$ Hz. (b) $f = 1$ kHz. (c) $f = 10$ kHz. (d) $f = 100$ kHz.

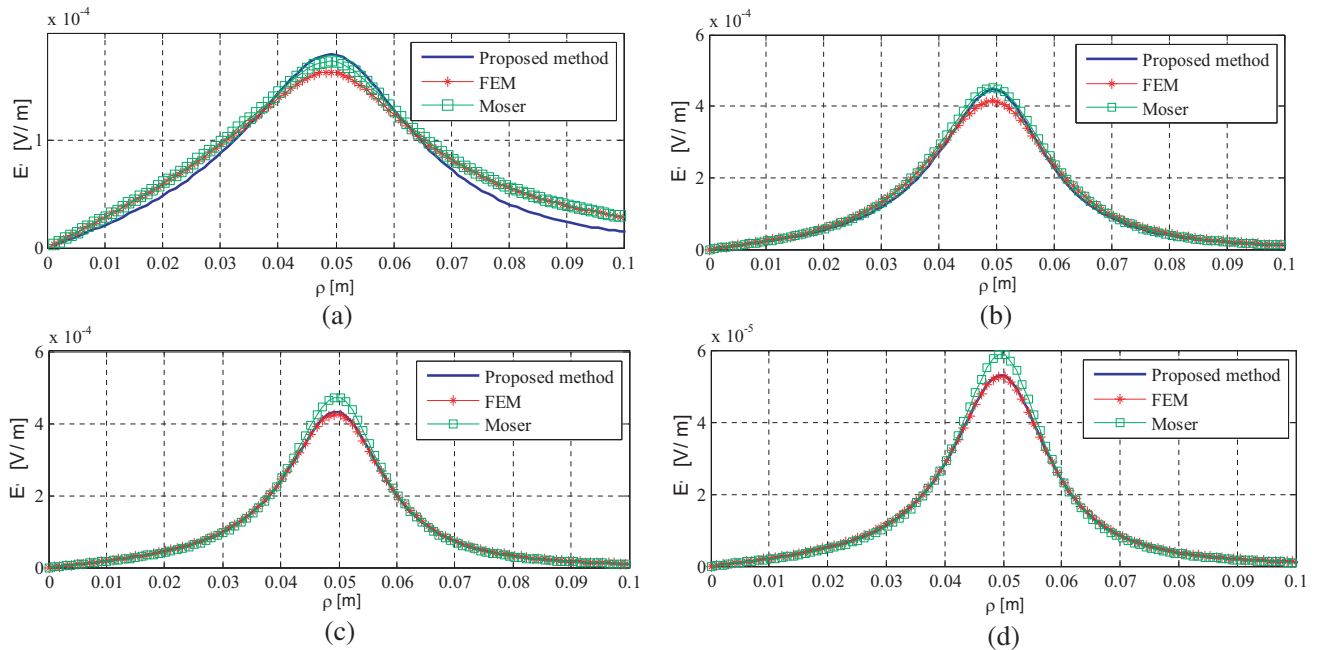


Figure 7. Complex magnitude of electric field tangential component $E = E_\varphi$ calculated at $\zeta = t$ for various frequencies along the radial distance ρ assuming $d = 10$ mm and $t = 1$ mm. (a) $f = 100$ Hz. (b) $f = 1$ kHz. (c) $f = 10$ kHz. (d) $f = 100$ kHz.

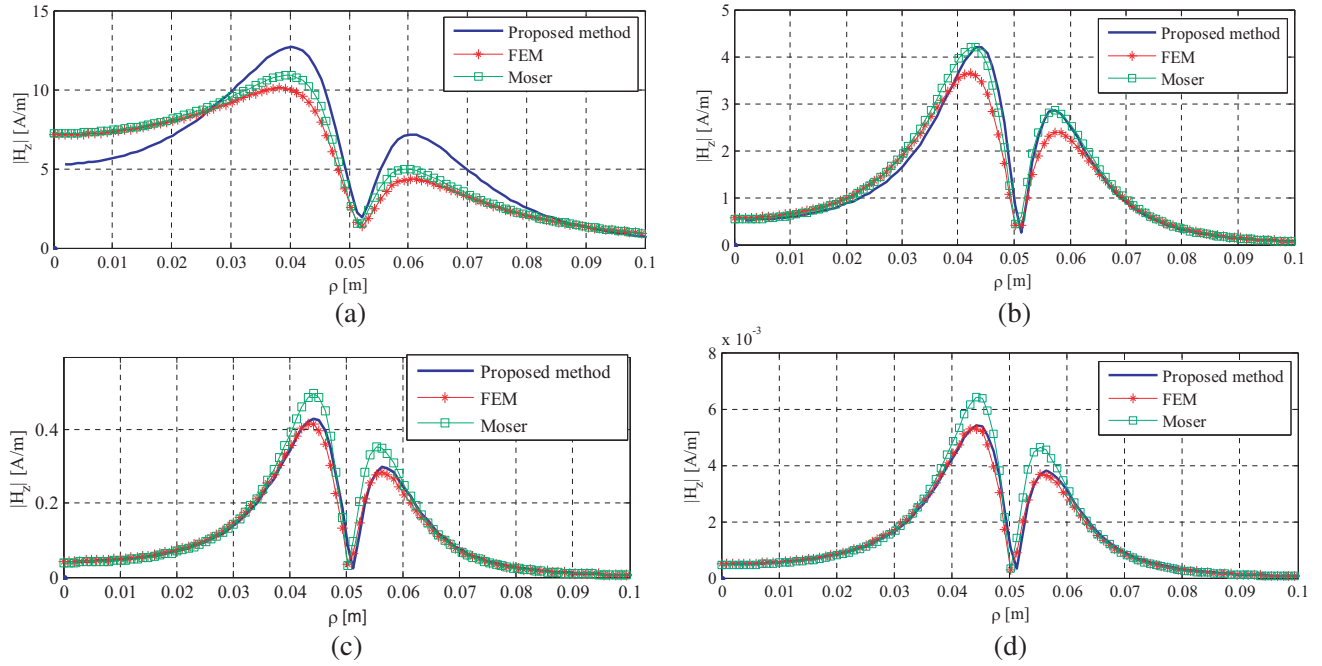


Figure 8. Complex magnitude of magnetic field normal component H_z calculated at $\zeta = t$ for various frequencies along the radial distance ρ assuming $d = 10$ mm and $t = 1$ mm. (a) $f = 100$ Hz. (b) $f = 1$ kHz. (c) $f = 10$ kHz. (d) $f = 100$ kHz.

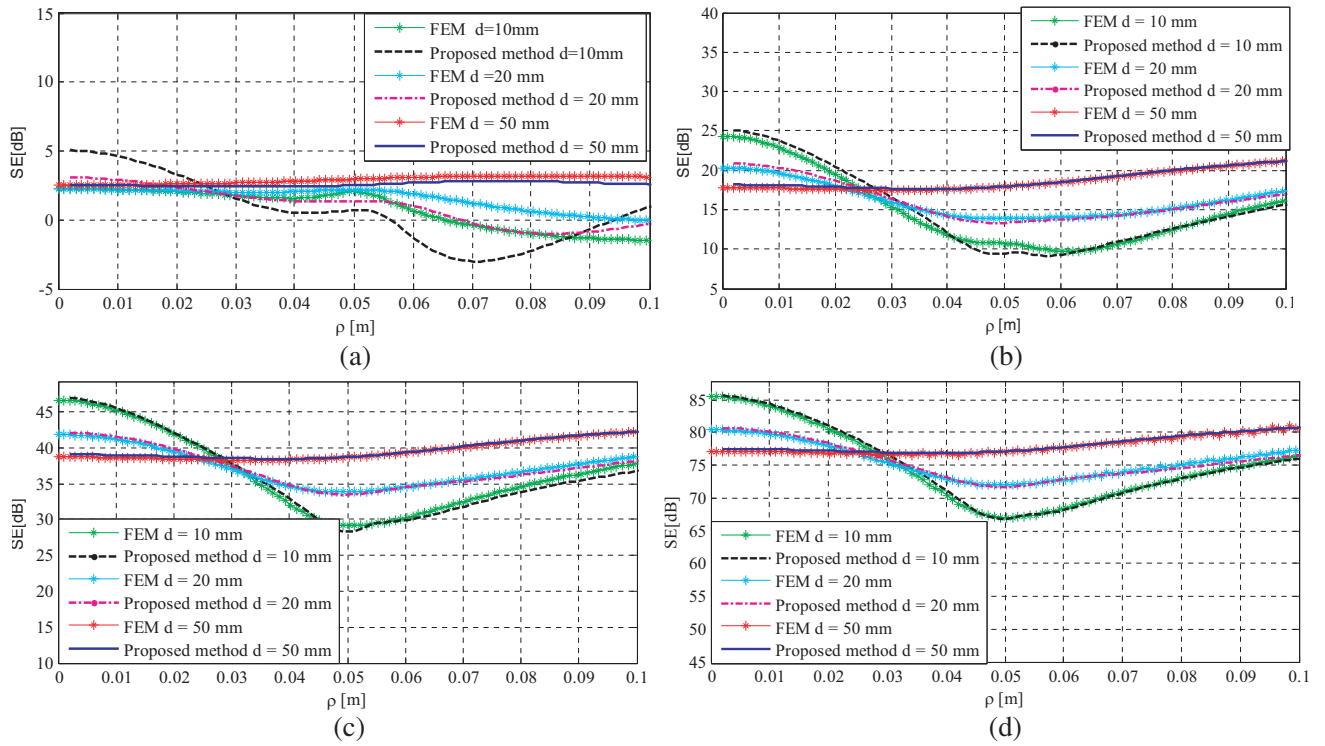


Figure 9. Shielding effectiveness SE_H calculated at various frequencies and various distances d along the radial distance ρ for $t = 1$ mm. (a) $f = 100$ Hz. (b) $f = 1$ kHz. (c) $f = 10$ kHz. (d) $f = 100$ kHz.

The proposed TL method solution is very accurate due to the use of the wave impedance of the total field components as right termination of the equivalent circuit. Thus it is interesting to note the differences between the wave impedances calculated by Eq. (9), as done by several authors, and by Eq. (10), as proposed in this paper. The behavior of $|Z_{w0}(\rho)|$ and $|Z_{wt}(\rho)|$ is shown in Fig. 10 for a copper planar shield assuming $f = 10$ kHz, $R = 5$ cm, $d = 10$ mm and $t = 1$ mm. Finally, it should be noted that the wave impedance calculated by Eq. (10) is affected by some approximations especially at higher frequencies since the axial variation of eddy currents within the shield is neglected in [2], but it is good enough to accurately evaluate the shielding effectiveness SE_H because the TL is terminated on a high impedance load.

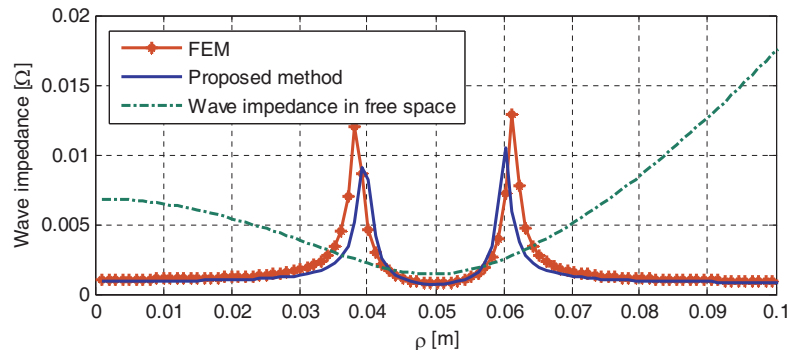


Figure 10. Complex magnitude of wave impedances along the radial distance ρ assuming $d = 10$ mm, $t = 1$ mm and $f = 10$ kHz.

4. CONCLUSIONS

The TL method is applied to predict shielding performance of a planar conductive shield in the presence of a circular loop current. Using the TL method, the magnetic shielding effectiveness is analytically calculated at any point on the shield surfaces. The novelty of the proposed TL method is in the terminal conditions of the equivalent circuit. Here, the load impedance is assumed to be the ratio of the tangential components of the total electric and magnetic fields instead of the incident fields, as proposed in the past by several authors without achieving good results. This modification permits to obtain very good results by analytical expressions. The proposed method is very efficient since it allows a fast and accurate prediction of the shielding effectiveness for magnetic near-field sources in a wide frequency range. Furthermore, the use of an equivalent circuit can permit an easy design of shielding for WPT coils. The proposed mathematical treatment is valid only for linear material shields. Finally, the proposed method is valid for an infinite planar shield, but it can be considered also valid for a finite extension shield whose dimensions are much larger than the coil radius.

REFERENCES

1. Schelkunoff, S. A., *Electromagnetic Waves*, Van Nostrand Company, New York, 1943.
2. Moser, J. R., "Low-frequency shielding of a circular loop electromagnetic field source," *IEEE Trans. Electromag. Compat.*, Vol. 9, No. 1, 6–18, Mar. 1967.
3. Moser, J. R. "Low-frequency low-impedance electromagnetic shielding," *IEEE Trans. Electromag. Compat.*, Vol. 30, No. 3, 202–210, Aug. 1988
4. Bannister, P. R., "New theoretical expressions for predicting shielding effectiveness for the plane shield case," *IEEE Trans. Electromag. Compat.*, Vol. 10, No. 1, 2–7, Mar. 1968.
5. Bannister, P. R., "Further notes for predicting shielding effectiveness for the plane shield case," *IEEE Trans. Electromag. Compat.*, Vol. 11, No. 2, 50–53, May 1969.
6. Whitehouse, A. C. D., "Screening: New wave impedance for the transmission-line analogy," *Proc. of IEEE*, Vol. 116, No. 7, 1159–1164, Jul. 1969.

7. Wait, J. R., "Image theory of a quasistatic magnetic dipole over a dissipative half-space," *Electronics Letters*, Vol. 5, No. 13, 281–282, Jun. 1969.
8. Nishikata, A. and A. Sugiura, "Analysis for electromagnetic leakage through a plane shield with an arbitrarily-oriented dipole source," *IEEE Trans. Electromag. Compat.*, Vol. 34, No. 3, 284–291, Aug. 1992.
9. Schultz, R. B., V. C. Plantz, and D. E. Brush, "Shielding Theory and Practice," *IEEE Trans. Electromag. Compat.*, Vol. 30, No. 3, 187–201, Aug. 1988.
10. Olsen, R. G., "Some observations about shielding extremely low-frequency magnetic fields by finite width shields," *IEEE Trans. Electromagn. Compat.*, Vol. 38, No. 3, 460–468, Aug. 1996.
11. Frix, W. M. and G. G. Karaday, "A circuital approach to estimate the magnetic field reduction of nonferrous metal shields," *IEEE Trans. Electromag. Compat.*, Vol. 39, No. 1, 24–32, Feb. 1997.
12. Du, Y., T. C. Cheng, and A. S. Farag, "Principles of power-frequency magnetic field shielding with flat sheets in a source of long conductors," *IEEE Trans. Electromag. Compat.*, Vol. 38, No. 3, 450–459, Aug. 1996.
13. Kurs, A., A. Karalis, R. Moffatt, J. D. Joannopoulos, P. Fisher, and M. Soljacic, "Wireless power transfer via strongly coupled magnetic resonances," *Science*, Vol. 317, No. 5834, 83–86, Jul. 2007.
14. Kim, J., J. Kim, S. Kong, H. Kim, I.-S. Suh, N. P. Suh, D.-H. Cho, J. Kim, and S. Ahn, "Coil design and shielding methods for a magnetic resonant Wireless Power Transfer system," *Proc. IEEE*, Vol. 101, No. 6, 1332–1341, Jun. 2013.
15. Cruciani, S. and M. Feliziani, "Mitigation of the magnetic field generated by a wireless power transfer (WPT) system without reducing the WPT efficiency," *EMC Europe — Int. Symposium on EMC*, Bruges, Belgium, Sept. 2–6, 2013.
16. Campi, T., S. Cruciani, and M. Feliziani, "Magnetic shielding of wireless power transfer systems," *EMC'14, /Tokyo, Proc of 2014 Int. Symp. Electromag. Compat.*, Tokyo, Japan, May 12–16, 2014.
17. Babic, S. I., J. Martinez, C. Akyel, and B. Babic, "Mutual inductance calculation between misalignment coils for wireless power transfer of energy," *Progress In Electromagnetics Research*, Vol. 38, 91–102, 2014.
18. Poon, A. S. Y., "A general solution to wireless power transfer between two circular loop," *Progress In Electromagnetics Research*, Vol. 148, 171–182, 2014.
19. Campi, T., S. Cruciani, V. De Santis, and M. Feliziani, "EMF safety and thermal aspects in a pacemaker equipped with a wireless power transfer system working at low frequency," *IEEE Trans. Microw. Th. Techn.*, Vol. 64, No. 2, 375–382, Feb. 2016.
20. Campi, T., S. Cruciani, V. De Santis, F. Palandrani, A. Hirata, and M. Feliziani, "Wireless power transfer charging system for AIMDs and pacemakers," *IEEE Trans. Microw. Th. Techn.*, Vol. 64, No. 2, 633–642, Feb. 2016.
21. Simpson, J. C., J. E. Lane, C. D. Immer, and R. C. Youngquist, "Simple analytic expressions for the magnetic field of a circular current loop," *NASA Technical Report 2001*, NASA/TM-2013-217919, Available online: <http://ntrs.nasa.gov/search.jsp?R=20140002333>.
22. Griffith, J. M. and G. W. Pan, "Time harmonic fields produced by circular current loops," *IEEE Trans. Magnetics*, Vol. 47, No. 8, 2029–2033, Aug. 2011.
23. Balanis, C. A., *Antenna Theory: Analysis and Design*, 3rd Edition, J. Wiley, NY, 2005.
24. Celozzi, S., R. Araneo, and G. Lovat, *Electromagnetic Shielding*, J. Wiley, Wiley Interscience, Hoboken, NJ, 2008.
25. Feliziani, M., F. Maradei, and G. Tribellini, "Field analysis of penetrable conductive shields by the Finite-Difference Time-Domain Method with Impedance Network Boundary Conditions (INBC's)," *IEEE Trans. Electromag. Compat.*, Vol. 41, No. 4, 307–319, Nov. 1999.
26. Buccella, C., M. Feliziani, F. Maradei, and G. Manzi, "Magnetic field computation in a physically large domain with thin metallic shields," *IEEE Trans. Magnetics*, Vol. 41, No. 5, 1708–1711, May 2005.
27. Feliziani, M., "Subcell FDTD modeling of field penetration through lossy shields," *IEEE Trans. Electromag. Compat.*, Vol. 54, 299–307, 2012.